APSB
2019

ORIGINAL ARTICLE

Development of the triazole-fused pyrimidine derivatives as highly potent and reversible inhibitors of histone lysine specific demethylase 1 (LSD1/KDM1A)

Zhonghua Li[a,c,d,†], Lina Ding[a,c,d,†], Zhongrui Li[a,c,d,†], Zhizheng Wang[a,c,d], Fengzhi Suo[a,c,d], Dandan Shen[a,c,d], Taoqian Zhao[a,c,d], Xudong Sun[a,c,d], Junwei Wang[a,c,d], Ying Liu[a,c,d], Liying Ma[a,c,d], Bing Zhao[a,c,d], Pengfei Geng[a,c,d], Bin Yu[a,b,c,d,*], Yichao Zheng[a,c,d,*], Hongmin Liu[a,c,d,*]

[a]School of Pharmaceutical Sciences, Zhengzhou University, Zhengzhou 450001, China
[b]State Key Laboratory of Pharmaceutical Biotechnology, Nanjing University, Nanjing 210023, China
[c]Co-Innovation Center of Henan Province for New Drug R&D and Preclinical Safety, Zhengzhou 450001, China
[d]Key Laboratory of Advanced Drug Preparation Technologies, Ministry of Education of China, Zhengzhou 450001, China

Abstract Histone lysine specific demethylase 1 (LSD1) has been recognized as an important modulator in post-translational process in epigenetics. Dysregulation of LSD1 has been implicated in the development of various cancers. Herein, we report the discovery of the hit compound **8a** (IC$_{50}$ = 3.93 μmol/L) and further medicinal chemistry efforts, leading to the generation of compound **15u** (IC$_{50}$ = 49 nmol/L, and K_i = 16 nmol/L), which inhibited LSD1 reversibly and competitively with H3K4me2, and was selective to LSD1 over MAO-A/B. Docking studies were performed to rationalize the potency of

compound **15u**. Compound **15u** also showed strong antiproliferative activity against four leukemia cell lines (OCL-AML3, K562, THP-1 and U937) as well as the lymphoma cell line Raji with the IC$_{50}$ values of 1.79, 1.30, 0.45, 1.22 and 1.40 μmol/L, respectively. In THP-1 cell line, **15u** significantly inhibited colony formation and caused remarkable morphological changes. Compound **15u** induced expression of CD86 and CD11b in THP-1 cells, confirming its cellular activity and ability of inducing differentiation. The findings further indicate that targeting LSD1 is a promising strategy for AML treatment, the triazole-fused pyrimidine derivatives are new scaffolds for the development of LSD1/KDM1A inhibitors.

1. Introduction

Histone modifications such as methylation, phosphorylation, acetylation, ubiquitylation, and sumoylation are thought to regulate transcription, chromatin structure and other nuclear processes[1,2]. Among them, the post-translational histone methylation is an important chromatin modification that is known to affect many biological processes[3]. To date, two classes of lysine demethylases (KDMs), namely KDM1s and JmjC KDMs, have been identified to be able to remove methyl groups of *N*-methyllysine residues through the flavin adenine dinucleotide (FAD) or Fe(II)/a-ketoglutarate (α-KG)-dependent oxidative mechanisms, respectively[4,5]. Although evidence of reversible methylation of calf thymus histones was documented by Kim and co-workers in 1973[6], the histone methylation had generally been recognized as an irreversible modification until the lysine specific histone demethylase 1 (LSD1 or KDM1A) was first identified by Shi and co-workers in 2004[7].

LSD1 catalyzes the demethylation of mono- and di-methylated K4 or K9 on histone H3 (H3K4me1/2 & H3K9me1/2) under diverse biological settings *via* the FAD-dependent enzymatic oxidation[8,9]. LSD1 could also remove methyl groups of non-histone substrates such as p53, E2F transcription factor, DNA methyltransferases (DNMTs) and further modulate their downstream cellular functions[10–14]. *In vivo*, LSD1 played a pivotal role during the process of early embryonic development and differentiation of embryonic stem cell[10,15–17]. By modulating the expression of target genes, LSD1 is closely associated with tumorigenesis[18], pluripotent stem cells[19], and neurodegenerative disorders[20,21]. Moreover, LSD1 has been observed to be over-expressed in various malignant tumors[22–29] and is closely associated with differentiation, proliferation, migration, invasion and poor prognosis[30,31]. Knockdown of *LSD1* using shRNA reduced glioma stem cells (GSCs) stemness and induced the differentiation. Pharmacological inhibition of LSD1 using NCL-1 and NCD-38 significantly reduced the cell viability, neurosphere formation and induced apoptosis of GSCs[32]. LSD1 has also been reported to able to promote S-phase entry and tumorigenesis *via* chromatin co-occupation with E2F1 and selective H3K9 demethylation[33]. These findings unveil the biological importance of LSD1 and the therapeutic potentials of LSD1 inhibitors.

To date, TCP-based LSD1 inhibitors ORY-1001/RG-6016, GSK2879552 (Clinicaltrials.gov identifier: NCT02177812) and INCB059872 (Clinicaltrials.gov identifier: NCT02712905) alone or in combination with other therapeutic agents such as all-trans retinoic acid (ATRA), cytarabine or azacitidine, etc., have advanced into clinical trials for the treatment of acute myeloid leukemia and small-cell lung cancer, etc. (Fig. 1)[34–36]. The success of TCP-based drug candidates makes TCP an attractive scaffold for the development of new LSD1 inhibitors[37]. Apart from TCP-based inhibitors, varieties of other different classes of LSD1 inhibitors have also been identified. However, these LSD1 inhibitors (*e.g.*, TCP, SP-2509, and GSK-690) have showed poor specificity, off-target effects, etc. For example, polyamine derived LSD1 inhibitors generally showed a low micromolar range and poor selectivity[38,39]. The highly potent hydrzone derivatives suffered from the off-target issues due to its slow response to CD86, an important biomarker of LSD1 activity[40]. In addition, pyridine-derived compound GSK-690 was reported to inhibit the human ether-a-go-go-related gene (*hERG*) cardiac ion channel, albeit with good anti-LSD1 potency in biochemical and cellular level[41,42].

Following our previous work on the identification of reversible LSD1 inhibitors[43–47], here we describe the identification of triazole-fused pyrimidine-based reversible LSD1 inhibitors through the biochemical screening of our in-house structurally diverse molecular library (*ca.* 500 compounds) and subsequent extensive medicinal chemistry efforts, leading to the identification of highly potent and selective LSD1 inhibitors (Fig. 2). Our data indicate that the triazole-fused pyrimidine is a new scaffold for the development of highly potent and selective LSD1 inhibitors.

2. Results and discussion

2.1. Synthetic routes

The synthetic routes of the designed compounds were presented in Schemes 1–4. The key intermediate derivatives **7a–ab** were
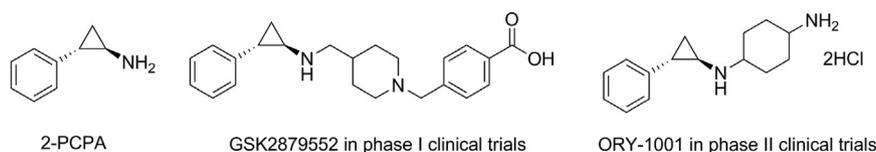

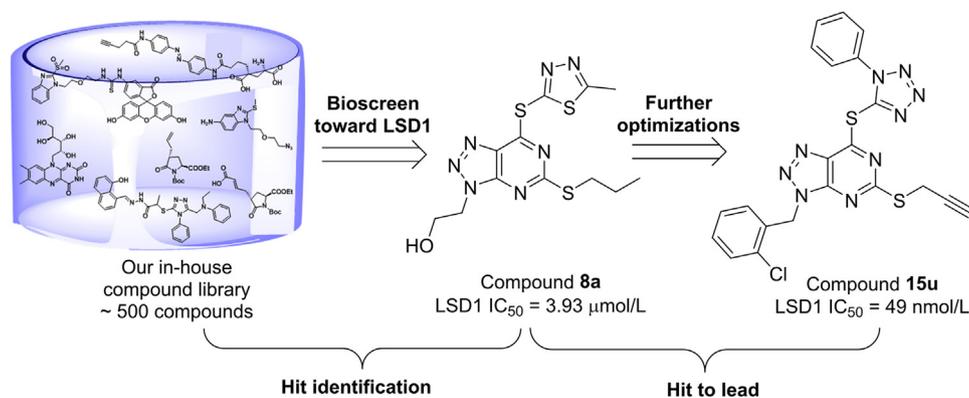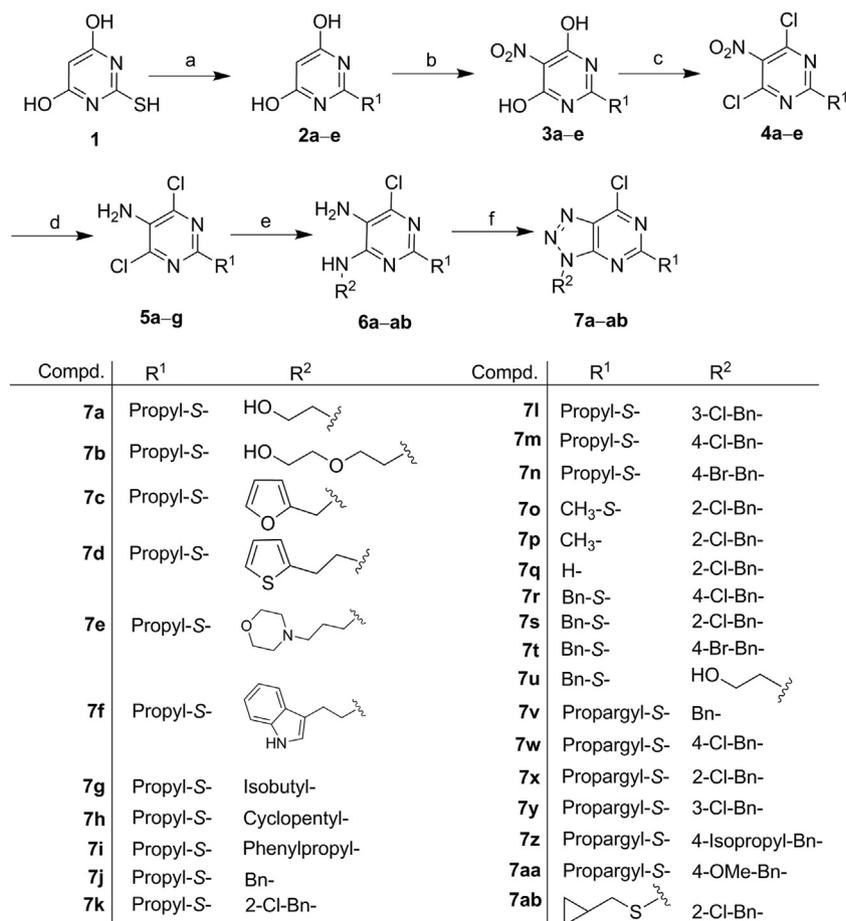**Figure 1** TCP-based LSD1 inhibitors.

Figure 2 Identification of hit compound **8a** from our chemical library and further optimizations leading to discovery of compound **15u**.

| Compd.	R^1	R^2	Compd.	R^1	R^2
7a	Propyl-S-	HO⌇	7l	Propyl-S-	3-Cl-Bn-
7b	Propyl-S-	HO⌇O⌇	7m	Propyl-S-	4-Cl-Bn-
7c	Propyl-S-	furanyl-CH₂	7n	Propyl-S-	4-Br-Bn-
7d	Propyl-S-	thienyl-CH₂	7o	CH₃-S-	2-Cl-Bn-
			7p	CH₃-	2-Cl-Bn-
7e	Propyl-S-	morpholinyl-propyl	7q	H-	2-Cl-Bn-
			7r	Bn-S-	4-Cl-Bn-
			7s	Bn-S-	2-Cl-Bn-
7f	Propyl-S-	indolyl-ethyl	7t	Bn-S-	4-Br-Bn-
			7u	Bn-S-	HO⌇
			7v	Propargyl-S-	Bn-
			7w	Propargyl-S-	4-Cl-Bn-
7g	Propyl-S-	Isobutyl-	7x	Propargyl-S-	2-Cl-Bn-
7h	Propyl-S-	Cyclopentyl-	7y	Propargyl-S-	3-Cl-Bn-
7i	Propyl-S-	Phenylpropyl-	7z	Propargyl-S-	4-Isopropyl-Bn-
7j	Propyl-S-	Bn-	7aa	Propargyl-S-	4-OMe-Bn-
7k	Propyl-S-	2-Cl-Bn-	7ab	cyclopropyl-CH₂-S-	2-Cl-Bn-

Scheme 1 Synthesis of Intermediates **7a–ab**. Reagents and conditions: (a) alkyl bromide, TEA, MeOH, reflux, 2 h; (b) fuming nitric acid, AcOH, 25–45 °C, 1 h; (c) POCl₃, DMA, reflux, 2 h; (d) Fe, AcOH, MeOH, reflux; (e) appropriate amines, TEA, EtOH, reflux, 48 h; (f) NaNO₂, AcOH, H₂O, 10 °C, 1 h.

prepared following our previously reported procedures, as depicted in Scheme 1[48]. Briefly, treatment of 2-mercaptopyrimidine-4,6-diol (**1**) with alkyl bromide in MeOH gave compound **2a–e**, which then reacted with fuming nitric acid, affording compounds **3a–e**. Chlorination of **3a–e** using POCl₃ yielded **4a–e**, which was then subjected to Fe-mediated hydrogenation, generating compounds **5a–g**. Compounds **5a–g** reacted with different amines in the presence of triethylamine (TEA) in EtOH to form compounds **6a–ab**, which were then treated with NaNO₂, generating the

intermediates **7a–ab**, in which the new triazole ring was formed efficiently.

As shown in Scheme 2A, compounds **8a–l** were efficiently synthesized from compounds **7a–b** in the presence of TEA through the nucleophilic substitution reactions of different mercapto heterocyclic analogs. Compounds **8k** and **8l** were then chosen for further modifications by reacting with 4-toluenesulfonyl chloride (TsCl), methanesulfonyl chloride (MsCl), benzoyl chloride (BzCl), respectively, affording compounds **9a–b** and **10** (Scheme 2B).
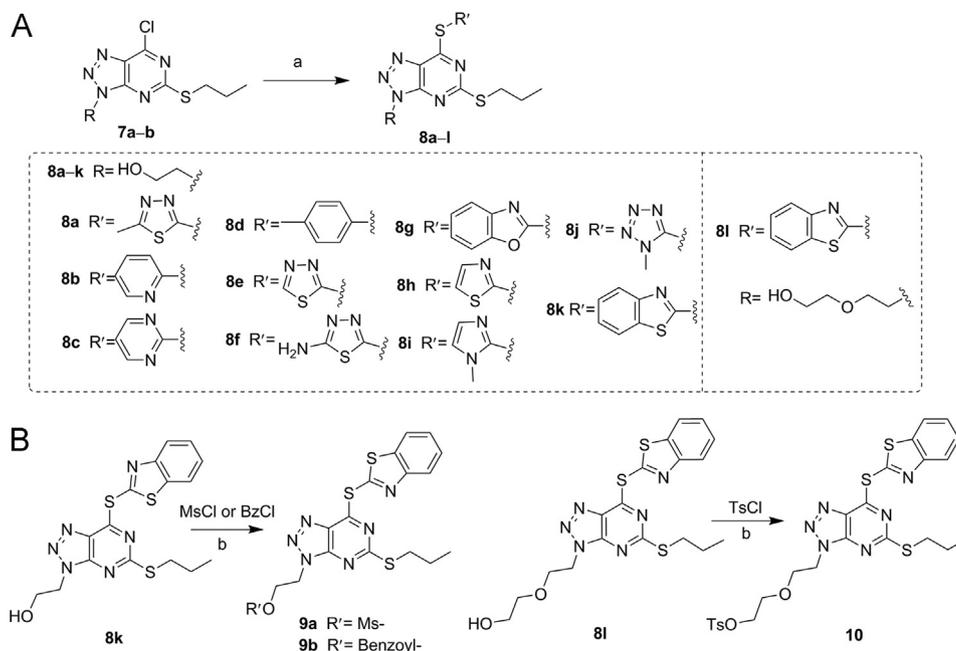
Scheme 2 Synthesis of compounds **8a–l**, **9a–b** and **10**. Reagents and conditions: (a) mercapto heterocyclic analogs, TEA, MeCN, reflux, 2 h; (b) TEA,DCM, rt, overnight.
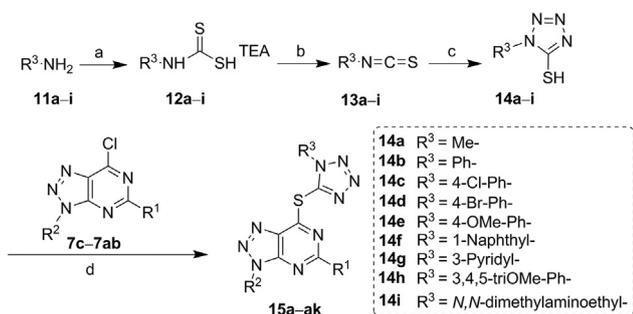
Scheme 3 Synthesis of compounds **15a–ak**. Reagents and conditions: (a) TEA or DABCO, CS_2, THF, rt, overnight; (b) BTC, $CHCl_3$, rt, overnight; (c) NaN_3, H_2O, reflux, 5 h; (d) TEA, MeCN, reflux, 2 h.

In addition, replacement of heterocycles in compounds **8a–k** with the tetrazole ring led to formation of compounds **15a–ak**. As shown in Scheme 3, the mercapto tetrazole derivatives **14a–i** were synthesized from amines **11a–i**. Aromatic amine reacted with carbon disulfide in the presence of TEA or triethylenediamine (DABCO) to produce dithiocarbamic acid salts **12a–i**[49], followed by addition of triphosgene (BTC) in chloroform to form isothiocyanates **13a–i**. Isothiocyanates **13a–i** reacted with sodium azide in water to give the mercaptotetrazole analogs **14a–i**, which then reacted with intermediates **7c–7ab** in the presence of TEA in MeCN to yield compounds **15a–ak**.

Furthermore, bioisosteric replacement and scaffold hopping have widely been recognized as two useful strategies in drug design, which have led to the identification of numerous lead compounds[50,51]. In this work, the triazole-fused pyrimidine scaffold was also replaced with the triazolo[5,4-d]pyrimidine, purine and pyrimidine scaffold, respectively, forming the corresponding compounds **17**, **19**, **22a–b** and **23**. As shown in Scheme 4, treatment of compound **4b** with phenyl isothiocyanate in the presence of Cs_2CO_3 in MeCN gave compound **16**, which then

reacted with 5-mercapto-1-methyltetrazole to afford compound **17** (Scheme 4A). Compound **6j** was chosen as the starting material for constructing the purine scaffold **18** by reacting with triethoxy methane (Scheme 4B). The nucleophilic substitution reaction of 5-mercapto-1-methyltetrazole with compound **18** yielded compound **19**. Compounds **20a–b** reacted with 5-mercapto-1-phenyltetrazole in the presence of DIEA in DMF to generate compounds **21a–b**, followed by the substitution reaction with 2-aminoethanol to yield **22a–b** (Scheme 4C). The terminal alkyne group of compound **22a** was then employed to synthesize compound **23** bearing an additional triazole moiety via the copper-catalyzed azide-alkyne cycloadditions (CuAAC) (Scheme 4D). Conceivably, more analogs of compound **23** could be obtained from different alkynes through the CuAAC reactions and could be used to construct compound collections.

2.2. LSD1 inhibitory activity and structure–activity relationship studies (SARs)

All the compounds synthesized in this study were examined for their in vitro inhibitory effect toward LSD1, and GSK2879552 was chosen as a positive control[46,47]. The results were summarized in Tables 1–4. Besides, to avoid interference of false positive compounds, PAINS screening of the synthesized compounds was carried out by employing the online program ("PAINS-Remover", http://www.cbligand.org/PAINS/)[52], and all the tested compounds passed the filter.

The hit compound **8a** identified from our in-house library inhibited LSD1 moderately with an IC_{50} value of 3.93 μmol/L. This interesting result promoted us to perform further structural elaborations. Replacement of the thiadiazole ring in **8a** with other aromatic rings led to the formation of compounds **8b–k** (Table 1). Clearly, compounds **8d** and **8i** bearing the phenyl and imidazole ring, respectively were found to be inactive toward LSD1 ($IC_{50} > 10$ μmol/L). The remaining compounds showed acceptable inhibitory effect toward LSD1 with the IC_{50} values less
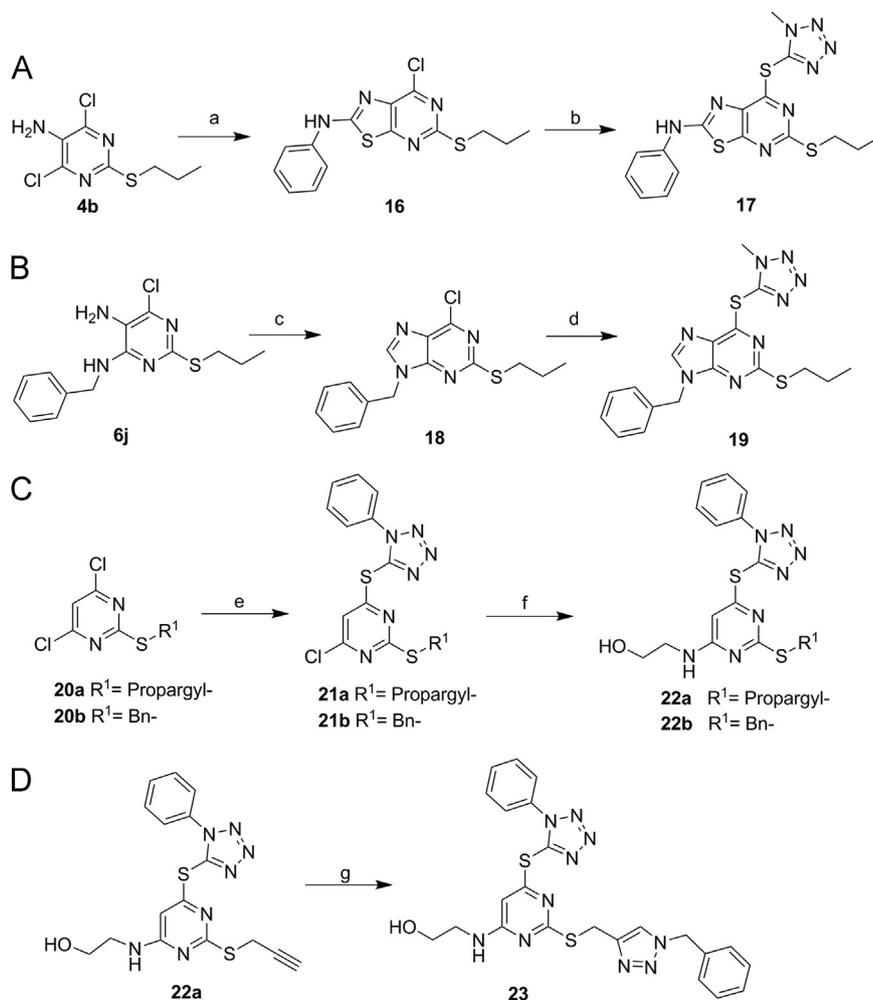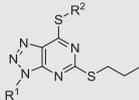
Scheme 4 Synthesis of compounds **17**, **19**, **22a–b** and **23**. Reagents and conditions: (a) PhSCN, Cs₂CO₃, MeCN, rt, overnight; (b) 5-mercapto-1-methyltetrazole, K₂CO₃, *i*-PrOH, reflux, 5 h; (c) CH(OEt)₃, aq HCl, rt, 8 h; (d) 5-mercapto-1-methyltetrazole, DIEA, DMF, 100 °C, 3 h; (e) 5-mercapto-1-phenyltetrazole, DIEA, DMF, 100 °C, 2 h; (f) DIEA, *i*-PrOH/DMF (*v/v*, 1:1), 90 °C, 3 h; (g) BnN₃, CuSO₄·5H₂O, sodium ascorbate, THF/H₂O (1:1), rt, 3 h.

than 9.0 μmol/L. Particularly, compounds **8j–k** possessing the tetrazole and benzothiazole, respectively, exhibited potent inhibition toward LSD1 with the IC₅₀ values of 0.60 and 0.85 μmol/L, respectively. Further derivatizations based on the hydroxy group of compound **8k** were carried out, yielding compounds **9a–b**, **8l** and **10**. Except for compound **9b**, compounds **9a**, **8l** and **10** also exerted moderate inhibitory effect, albeit with relatively lower activity than compound **8k**, suggesting the importance of the scaffold for the inhibitory activity.

The first round structural modifications as shown in Table 1 led to the identification of the tetrazole containing compound **8j**, which inactivated LSD1 potently (IC₅₀ = 0.60 μmol/L). Further structural optimizations centering on variations of R¹ and R² groups attached to the triazole–pyrimidine core were carried out, leading to the discovery of compounds **15a–s**. Interestingly, this series of compounds showed potent inhibition toward recombinant LSD1. Compound **15p** showed the best potency with an IC₅₀ value of 80 nmol/L, about 7.5-fold more potent than **8j**. For compounds **15a–l** bearing the same propylthio group (R¹), only compound **15e** bearing a hydrophilic morpholine group (R²) was found to have significantly decreased inhibitory effect toward LSD1 with an IC₅₀ value of 2.09 μmol/L, the remaining

compounds bearing a hydrophobic R² group exhibited comparable and potent inhibitory activity against LSD1. These findings reveal the essential structural elements for the activity toward LSD1. Replacement of the R¹ group with benzylthio, methylthio, methyl, hydrogen atom (H) and propargylthio groups led to a new series of compounds **15m–s**, of which compounds **15p** and **15s** inhibited LSD1 with the IC₅₀ value of 80 and 100 nmol/L, respectively. Interestingly, bioisosteric replacement of the triazole–pyrimidine in compounds **15a–s** with the thiazolo [5,4-*d*]pyrimidine and purine rings led to significantly decreased inhibitory activity. Compounds **17** and **19** were found to be inactive against LSD1 (IC₅₀ > 10 μmol/L).

Based on above findings, further modifications were mainly focused on variations of R³ group attached to the tetrazole ring. As shown in Table 3, this series of compounds generally exhibited excellent inhibition toward LSD1. Compound **15t** inactivated LSD1 with an IC₅₀ value of 0.15 μmol/L. While 2-chloro-benzyl (R²)-substituted compound **15u** exhibited about 3-fold increase in potency (IC₅₀ = 49 nmol/L), comparable to that of compound **15x** bearing 4-isopropy benzyl group (IC₅₀ = 55 nmol/L). Compounds **15v** and **15w** bearing the 3-Cl benzyl or 4-Cl benzyl group, respectively also displayed acceptable potency at nanomolar levels

Table 1 Inhibitory effect of compounds **8a–l**, **9a–b**, **10** and **11** on recombinant LSD1.

Compd.	R¹	R²	Inhibition at 10 μmol/L[a]	IC$_{50}$(μmol/L)[b]
8a	HO~	thiazole-CH₃	94.1%	3.93±0.26
8b	HO~	pyridyl	88.2%	2.63±0.40
8c	HO~	pyrimidinyl	55.7%	8.90±0.30
8d	HO~	phenyl	28.3%	>10
8e	HO~	thiadiazole	90.1%	1.05±0.09
8f	HO~	H₂N–thiadiazole	78.4%	2.10±0.03
8g	HO~	benzoxazole	89.4%	2.54±0.36
8h	HO~	thiazole	93.0%	1.03±0.01
8i	HO~	imidazole(N-CH₃)	40.3%	>10
8j	HO~	triazole(N-CH₃)	87.1%	0.60±0.07
8k	HO~	benzothiazole	89.6%	0.85±0.09
9a	MsO~	benzothiazole	79.5%	3.15±0.20
9b	Ph–C(O)O~	benzothiazole	44.5%	>10
8l	HO~O~	benzothiazole	88.4%	1.39±0.08
10	TsO~O~	benzothiazole	68.1%	6.37±1.01
GSK2879552	–	–	–	0.038±0.007

[a]Data are represented as the mean of the inhibition rate.
[b]Data are represented as mean ± SD. All experiments were independently carried out at least three times.
– Not applicable.

(IC$_{50}$ = 74 and 93 nmol/L, respectively), but was slightly less potent than **15t**. 4-Methoxyl-benzyl-substituted compound **15y** showed slightly decreased activity against LSD1 with an IC$_{50}$ value of 140 nmol/L, comparable to that of compound **15t**. In contrast, compounds **15z** and **15aa** with a larger benzylthio group (R¹) exhibited remarkably decreased inhibitory activity (IC$_{50}$ = 300 and 410 nmol/L, respectively). Compared with compound **15u**, compound **15ac** exerted decreased inhibitory activity with the steric hindrance of R¹ group increased correspondingly. When the R³ substitution was substituted with phenyl ring, naphthyl or pyridyl group, the corresponding compounds **15ad–ai** showed decreased activity. Particularly, when the R³ group was the hydrophilic *N,N*-dimethylaminoethyl group, compound **15aj** was found to be inactive against LSD1.

Finally, the scaffold hopping strategy was employed to investigate the effects of the core scaffold variations on the LSD1 inhibition, and compounds **15ak**, **22b** and **33** were produced and compared. As shown in Table 4, the removal of the triazole ring of compound **15ak** led to the generation of compound **22b**, which was found to be inactive toward LSD1 (IC$_{50}$ > 10 μmol/L),

highlighting the importance of the triazole-fused pyrimidine scaffold for the activity. Additionally, compound **23** bearing a triazole ring at the side chain also showed weak inhibition toward LSD1 (36.3% inhibitory rate at 10 μmol/L).

2.3. Molecular docking studies of LSD1 inhibitors

We carried out a molecular docking study to predict the possible binding mode of the studied compounds with LSD1 using MOE 2015.10. The crystal structure of LSD1 in complex with an H3K4 peptide (PDB code: 2V1D) was used as receptor protein, and was prepared by adding hydrogen atoms, removing water molecules and the peptide, while FAD was kept as a component of the receptor. Docking results showed that the 20 binding structures with the lowest-energies of the most potent compound **15u** were similar (Fig. 3A). The tetrazole ring formed hydrogen bond interactions with the side chain of Gln358 and Asn535. The distance of these two hydrogen bonds was 2.7 and 2.5 Å respectively. The phenyl group attached to the tetrazole ring was surrounding by Ile356, Leu677 and Trp695, and had hydrophobic interactions with these residues (Fig. 3B). The triazole ring formed a hydrogen bond as well as electrostatic interaction with the positively charged side chain of His564, and the distance was 2.7 Å. The pyrimidine ring was predicted to form a hydrogen bond with the side chain of Asn535 while the distance was 2.4 Å. The 2-Cl phenyl group would be located at the hydrophobic pocket that consists of the flavin ring of FAD, Val333, Phe538, Trp695 and Tyr761, and had π–π stacking with flavin ring, Phe538, Trp695 and Tyr761. In addition, the propargyl group had hydrophobic interactions with Phe382, Leu536 and Trp552 (Fig. 3C). The docking results predicted the binding models of compound **15u** in the active site of LSD1, and could well explain the activity discrepancy of our synthesized compounds. The hydrogen bond and strong electrostatic interaction with the positively charged side chain of His564 could explain the importance of triazole ring. Replacement of the triazole ring with thiazole or imidazole may lead to the decrease of hydrogen interaction and electrostatic interaction, which may be responsible for the loss of the anti-LSD1 activity of compounds **17**, **19**, **22b** and **23**. Besides, the substituent connecting with the triazole ring was predicted to locate at a hydrophobic pocket and had π–π stacking with some surrounding residues, which could account for the increased activity of compound **15u** compared to **8j** with hydroxyethyl side chain. Interestingly, the replacement of the phenyl ring with the hydrophilic *N,N*-dimethylaminoethyl group caused the complete loss of the activity (compound **15u** *vs.* compound **15aj**), suggesting the essential structural element for the anti-LSD1 activity. In addition, a newly released crystal structure of LSD1-CoREST in complex with a small molecular inhibitor (4-[5-(piperidin-4-ylmethoxy)-2-(*p*-tolyl)pyridin-3-yl]benzonitrile, PDB code: 5YJB) was also employed for binding mode prediction (Fig. 3D), presenting a quite similar docking result with that (Fig. 3B) generated from protein receptor (PDB 2V1D). The 3D-QSAR model was also established based on the data of this series (Supporting Information Tables S1, S2 and Fig. S1), which may provide directions for designing new potent and selective LSD1 inhibitors.

2.4. Selectivity and reversibility of compound **15u**

As LSD1 belongs to the monoamine oxidases (MAOs) family, the most potent LSD1 inhibitor compound **15u** (IC$_{50}$ = 49 nmol/L, K_i = 16 nmol/L, Fig. 4A) was then examined for its enzymatic selectivity against MAO-A and MAO-B. As showed in Fig. 4B,

Table 2 Inhibitory effect of compounds **15a–s**, **17** and **19** on recombinant LSD1.
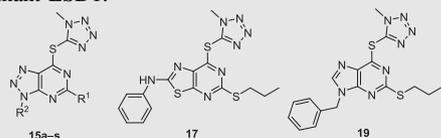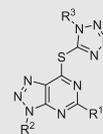

Compd.	R^2	R^1	IC$_{50}$(μmol/L)[a]
15a	(2-furyl-CH$_2$CH$_2$-)	Propyl-S-	0.45±0.11
15b	(2-thienyl-CH$_2$CH$_2$-)	Propyl-S-	0.34±0.01
15c	Isobutyl-	Propyl-S-	0.46±0.03
15d	Cyclopentyl-	Propyl-S-	0.41±0.02
15e	(morpholino-propyl-)	Propyl-S-	2.09±0.06
15f	(indolyl-ethyl-)	Propyl-S-	0.25±0.04
15g	Phenylpropyl-	Propyl-S-	0.15±0.01
15h	Bn-	Propyl-S-	0.21±0.02
15i	2-Cl-Bn-	Propyl-S-	0.16±0.05
15j	3-Cl-Bn-	Propyl-S-	0.29±0.01
15k	4-Cl-Bn-	Propyl-S-	0.19±0.01
15l	4-Br-Bn-	Propyl-S-	0.25±0.01
15m	4-Br-Bn-	Bn-S-	0.55±0.07
15n	4-Cl-Bn-	Bn-S-	0.36±0.01
15o	2-Cl-Bn-	Bn-S-	0.20±0.01
15p	2-Cl-Bn-	Me-S-	0.08±0.02
15q	2-Cl-Bn-	Me-	0.24±0.01
15r	2-Cl-Bn-	H-	0.18±0.03
15s	Bn-	Propargyl-S-	0.10±0.02
17	–	–	>10
19	–	–	>10
GSK2879552	–	–	0.038±0.007

[a]Data are represented as mean±SD. All experiments were independently carried out at least three times.
–, not applicable.

Table 3 Inhibitory effect of compounds **15t–aj** on recombinant LSD1.

Compd.	R^2	R^1	R^3	IC$_{50}$(μmol/L)[a]
15t	Bn-	Propargyl-S-	Ph-	0.15±0.001
15u	2-Cl-Bn-	Propargyl-S-	Ph-	0.049±0.004
15v	3-Cl-Bn-	Propargyl-S-	Ph-	0.074±0.012
15w	4-Cl-Bn-	Propargyl-S-	Ph-	0.093±0.011
15x	4-Isopropyl-Bn-	Propargyl-S-	Ph-	0.055±0.002
15y	4-OMe-Bn-	Propargyl-S-	Ph-	0.14±0.033
15z	4-Cl-Bn-	Bn-S-	Ph-	0.30±0.04
15aa	4-Br-Bn-	Bn-S-	Ph-	0.41±0.02
15ab	2-Cl-Bn-	Me-S-	Ph-	0.073±0.005
15ac	2-Cl-Bn-	(cyclopropyl-CH$_2$-S-)	Ph-	0.23±0.001
15ad	2-Cl-Bn-	Propargyl-S-	4-OMe-Ph-	0.76±0.02
15ae	2-Cl-Bn-	Propargyl-S-	3,4,5-triOMe-Ph-	0.97±0.04
15af	2-Cl-Bn-	Propargyl-S-	4-Cl-Ph-	0.48±0.07
15ag	2-Cl-Bn-	Propargyl-S-	4-Br-Ph-	1.77±0.21
15ah	2-Cl-Bn-	Propargyl-S-	1-Naphthyl-	0.15±0.03
15ai	2-Cl-Bn-	Propargyl-S-	3-Pyridyl-	0.13±0.002
15aj	2-Cl-Bn-	Propargyl-S-	N,N-dimethylaminoethyl	>10
GSK2879552	–	–	–	0.038±0.007

[a]Data are represented as mean±SD. All experiments were independently carried out at least three times.
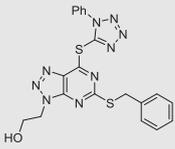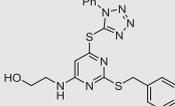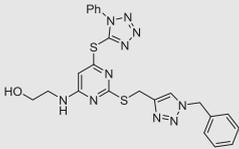–, not applicable.

reference compound (Supporting Information Table S3). As shown in Fig. 5, compound **15u** was found to be devoid of the inhibitory activity with <15% of the inhibitory rate at 10 μmol/L toward the tested kinases. The data indicated that compound **15u** was highly selective to LSD1 over the tested kinases.

2.6. Antiproliferative ability of compounds 15s, 15u and 15y

Compound **15u** was then tested for its antiproliferative ability of several LSD1-overexpressed cancer cell lines. As depicted in Table 5, treatment of compound **15u** for 6 days exhibited strong antiproliferative activity against the four leukemia cell lines (OCL-AML3, K562, THP-1 and U937) as well as the lymphoma cell line Raji with the IC$_{50}$ values of 1.79, 1.30, 0.45, 1.22 and 1.40 μmol/L, respectively. Clearly, THP-1 cell line was found to be more sensitive to compound **15u** as it harbors a t(9;11) translocation, the cytogenetic hallmark of MLL-AF9, while LSD1 acts at genomic loci bound by MLL-AF9 to sustain expression of the associated oncogenic program, thus preventing differentiation as reported[56]. Another two compounds **15s** and **15y** (LSD1 IC$_{50}$=100 and 140 nmol/L, respectively) also displayed strong antiproliferative activity against OCL-AML3, K562, THP-1, U937 and Raji at low micromolar levels and certain selectivity to THP-1 cells. In contrast, the reference compound GSK2879552 was found to be inactive toward THP-1 cells with an IC$_{50}$ of more than 50 μmol/L. The activity discrepancy may be due to that our compounds may also bind to other cellular targets. Further mechanistic studies are underway in our lab and will be reported in due course.

We next evaluated how LSD1 inhibitors altered the colony-forming capacity of THP-1 cells with soft agar assay, coupled with high content analysis. As indicated in Fig. 6A, treatment of compound **15u** for 8 days significantly inhibited colony formation of THP-1 cells. As

compound **15u** inhibited LSD1 with an inhibitory rate of 95.8% at 1 μmol/L, while it inhibited MAO-A/B with the inhibitory rates below 10% at 1 μmol/L and around 40% of inhibitory rates at 10 μmol/L, indicating that compound **15u** may be highly selective to LSD1 over MAO-A/B. Furthermore, the reversibility of compound **15u** against LSD1 was also investigated using the dilution assay. As shown in Fig. 4C, 80-fold dilution of the LSD1/compound **15u** complex resulted in more than 80% recovery of LSD1 activity, while the positive control GSK2879552 failed to recover the activity of LSD1. These results indicated that compound **15u** may interact with LSD1 in a reversible manner. Additionally, with classic Lineweaver–Burk plots, compound **15u** was characterized as a substrate (H3K4me2) competitive inhibitor over LSD1 (Fig. 4D), as compared to the noncompetitive and uncompetitive fitting (Supporting Information Fig. S2).

2.5. Kinase inhibition

Pyrimidine-containing bicyclic N-heterocycles have been reported to be inhibitors of a number of kinases, such as Bruton's tyrosine kinase (BTK) or cyclin-dependent kinases (CDKs)[53–55], herein compound **15u** was also evaluated against some selected kinases such as BTK and CDK1/2/4/6/7/9, and staurosporine was used as

Table 4 Inhibitory effect of compounds **15ak**, **22b** and **23** on recombinant LSD1.

Compd.	Structure	Inhibition at 10 μmol/L[a]	IC$_{50}$ (μmol/L)[b]
15ak		97.7%	0.54±0.01
22b		12.7%	>10
23		36.3%	>10
GSK2879552	–	–	0.038±0.007

[a]Data are represented as the mean of the inhibition rate.
[b]Data are represented as mean±SD. All experiments were independently carried out at least three times.

B7-2 (CD86), one of type I transmembrane proteins that were originally identified as ligands for CD28/CTLA-4, is a surrogate cellular biomarker of LSD1 activity[57], THP-1 cells were treated with compound **15u** to evaluate its effect on protein expression of CD86. As indicated in Fig. 6B, increased CD86 expression was observed, suggesting that compound **15u** may inactivate LSD1 in the cellular level. Moreover, considering that LSD1 inhibition could induce differentiation of human monocytic cells[58,59], the THP-1 monocytic cells line were treated with compound **15u** at three different concentrations to evaluate its effect on CD11b, a well-known myelo-monocytic differentiation marker modulated by KDM1A[60]. As shown in Fig. 6C, compound **15u** induced expression increase of CD11b in THP-1 cells concentration dependently, which suggests the differentiation induction of the THP-1 cells. Also, treatment of THP-1 cells with compound **15u** caused remarkable morphological changes of granulocytic differentiation[61], such as segmented nuclei and condensed chromatin (Fig. 6D).

3. Conclusions

In conclusion, we have reported the discovery of a series of triazole-fused pyrimidine derivatives as highly potent LSD1 inhibitors. Among them, the most potent compound **15u** (IC$_{50}$=49 nmol/L) inhibited LSD1 reversibly and competitively with H3K4me2 substrate, and showed selectivity to LSD1 over MAO-A/B. Molecular docking simulations and 3D-QSAR studies using the CoMFA model were performed to predict the binding models and to explain the SARs observed. The MTT assay indicated that compound **15u** exerted strong antiproliferative activity against four leukemia cell lines (OCL-AML3, K562, THP-1 and U937) and the lymphoma cell line Raji. Additionally, compound **15u** significantly inhibited colony

formation and caused remarkable morphological changes of THP-1 cells in a concentration-dependent manner. Compound **15u** also induced expression of CD86 and CD11b in THP-1 cells, confirming its cellular activity and ability of inducing differentiation. Taken together, compound **15u** is a newly developed heterocyclic inhibitor of LSD1, which makes the triazole-fused pyrimidine an attractive scaffold for the discovery of potent inhibitors of LSD1.

4. Experimental

4.1. Chemistry

Reagents and solvents were purchased from commercial sources and were used without further purification. All reaction were monitored by thin-layer chromatography (TLC) and visualized with UV light. Melting points were determined on an X-5 micromelting apparatus (Haohai Inc., Nanjing, China) and are uncorrected. ^{1}H NMR and ^{13}C NMR spectra were recorded on a Bruker 400 and 100 MHz spectrometer (Ettlingen, Germany), respectively. High resolution mass spectra (HR-MS) were recorded on a Waters Micromass Q-T of Micromass spectrometer (Milford, MA, USA) by electrospray ionization (ESI). Final products were of >95% purity as analyzed by HPLC analysis (Phenomenex column, C18, 5.0 μm, 150 mm × 4.6 mm) on Dionex UltiMate 3000 UHPLC instrument from ThermoFisher (Waltham, MA, USA). The signal was monitored at 254 nm with a UV dector. A flow rate of 1.0 mL/min was used with a mobile phase of methanol in H$_2$O (80:20, v/v).

4.1.1. Preparation of compound 5e

To a suspension of 2-mercaptobarbituricacid **1** (7 g, 48 mmol, 1 eq.) in methanol (40 mL) was added triethylamine (7 mL, 51 mmol, 1.05 eq.) at rt, and a clear solution was formed. Then cyclopropylmethyl bromide (4.7 mL, 48 mmol, 1 eq.) was added dropwise over 20 min and was kept stirring under reflux for 2 h. After cooling to rt, the formed precipitate was filtered and washed with methanol to afford compound **2e** (4.2 g, yield 44%), which was very smelly and used for the next step without further purification. The obtained compound **2e** was added cautiously in portions to a precooled solution of fuming nitric acid (3.6 mL) in acetic acid (11 mL) in an ice bath, and the resulting slurry was stirred for 1 h below 35 °C. After the completion of the reaction, the slurry was poured to crushed ice and stirred for 20 min. The precipitate was obtained by filtration and washed with water, affording compound **3e** as smelly pink solid (3.9 g, yield 76%) which was directly used for the next step. Then compound **3e** was dissolved in POCl$_3$ (10 mL) at rt, following the addition of N,N-dimethylphenylamine (3.5 mL). The reaction mixture was refluxed for 3 h and monitored by TLC (PE/EA = 5:1). After cooled to rt, the mixture was hydrolyzed by pouring on the crushed ice, and extracted with ethyl acetate. The organic phase was washed with water and saturated sodium bicarbonate. The solvent was evaporated under reduced pressure to afford crude product **4e**, which was used for the next step without further purification. To a mixture of acetic acid/ethanol (v/v = 1:5, 35 mL) was added compound **4e**, and followed by the addition of iron powder (2.7 g, 48 mmol) portionwise. The formed slurry was heated to 50 °C for 3 h, and monitored by TLC (PE/EA = 6:1). The reaction mixture was diluted with ethyl acetate, and filtrated over celite pad. The filtrate was washed with water and saturated sodium dicarbonate. The residue was purified by flash column chromatography (PE/EA
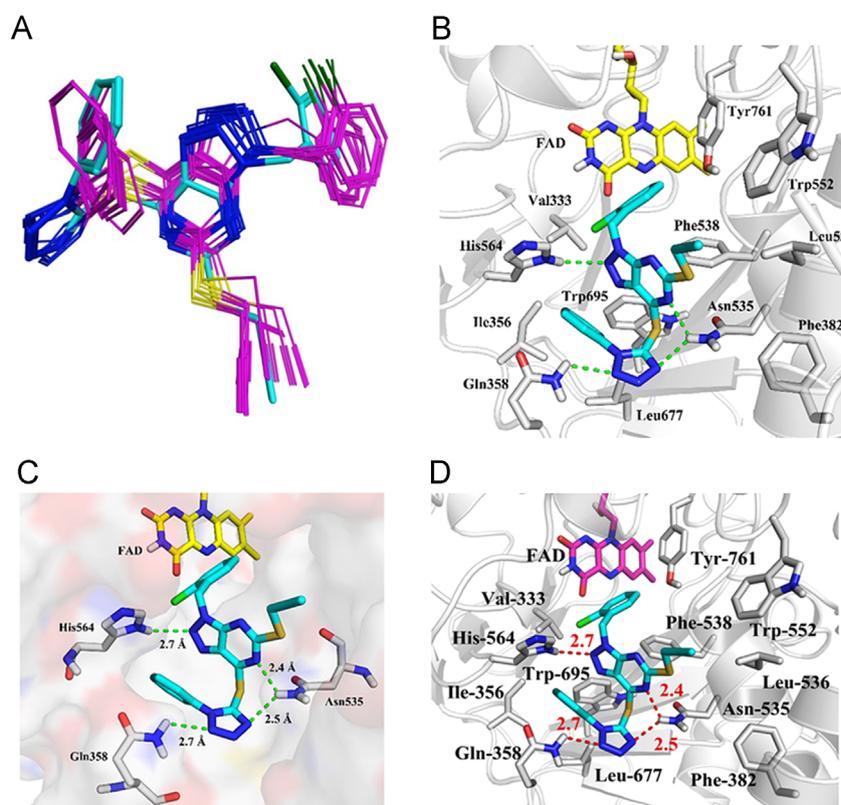
Figure 3 The proposed binding mode of compound **15u** with LSD1 (PDB code: 2V1D). (A) 20 lowest-energy docking structures of compound **15u**, with the most stable conformation shown as a cyan stick model; (B) Close-up views of the hydrogen bonds and hydrophobic interactions between compound **15u** and LSD1; (C) Close-up views of the hydrogen bond interactions between compound **15u** and LSD1; (D) The binding mode of compound **15u** with LSD1 (PDB code: 5YJB). Compound **15u** is shown in cyan stick representation, while the residues and FAD of LSD1 are shown in white and yellow stick representation, respectively.

= 6:1) to give compound **5e** as brown semi-solid, yield, 76%. ^{1}H NMR (400 MHz, CDCl$_3$) δ 4.21 (br, 2H), 3.05 (d, J = 7.2 Hz, 2H), 1.12–1.19 (m, 1H), 0.58–0.61 (m, 2H), 0.31–0.35 (m, 2H).

4.1.2. Preparation of compound 8a

The mixture of intermediate **7a** (1 eq.), 5-methyl-1,3,4-thiadiazole-2-thiol (1 eq.) and triethylamine (1.2 eq.) in 20 mL of acetonitrile was refluxed for 2 h and monitored by TLC. After completion of the reaction, the mixture was concentrated under reduced pressure. The residue was dissolved in ethyl acetate and washed with water successively. The crude product was purified by flash column chromatography on silica gel to afford compound **8a** as white solid, m.p. 111–112 °C, yield 65%. ^{1}H NMR (400 MHz, CDCl$_3$) δ 4.76–4.79 (t, J = 4.8 Hz, 2H), 4.22 (m, 2H), 3.09–3.12 (t, J = 7.4 Hz, 2H), 2.87 (s, 3H), 1.70–1.80 (m, 2H), 1.04–1.08 (t, J = 7.3 Hz, 3H). ^{13}C NMR (100 MHz, CDCl$_3$) δ 170.5, 169.1, 157.9, 155.0, 149.2, 130.9, 60.2, 50.2, 33.4, 22.1, 15.7, 13.5. HR-MS (ESI): Calcd. C$_{12}$H$_{15}$N$_7$OS$_3$, [M+H]$^+$: 370.0578, Found: 370.0567. Compounds **8b–l** and **15a–ak** were prepared through similar procedures as used for the synthesis of compound **8a** (see Supporting Information Section 6.2).

4.1.3. General procedure for the synthesis of compounds 9a–9b and 10

To a solution of compound **8k** (1 eq.) and triethylamine (1.1 eq.) in dry DCM was added methanesulfonyl chloride (1 eq.) in an ice

bath, then the reaction mixture was stirred at rt overnight. Upon completion, the reaction mixture was diluted with ethyl acetate and washed with water. The organic phase was dried over Na$_2$SO$_4$, and the solvent was removed under vacuum. The crude residue was purified by flash column chromatography (PE/EA = 3:1) to afford compound **9a** as white solid, yield 86%. Compounds **9b** and **10** were also synthesized following the same methods. m.p. 153–154 °C, ^{1}H NMR (400 MHz, CDCl$_3$) δ 8.12–8.14 (m, 1H), 7.97–7.99 (m, 1H), 7.55–7.59 (m, 1H), 7.49–7.53 (m, 1H), 4.95–4.97 (t, J = 5.2 Hz, 2H), 4.79–4.81 (t, J = 5.2 Hz, 2H), 3.00 (s, 3H), 3.00–2.96 (m, 2H), 1.55–1.62 (m, 2H), 0.85–0.89 (t, J = 7.4 Hz, 3H). ^{13}C NMR (100 MHz, CDCl$_3$) δ 171.3, 160.3, 154.9, 152.2, 149.2, 137.3, 131.1, 126.6, 126.1, 123.5, 121.3, 65.2, 46.1, 37.9, 33.5, 22.2, 13.3. HR-MS (ESI): Calcd. C$_{17}$H$_{18}$N$_6$O$_3$S$_4$, [M+Na]$^+$: 505.0221, Found: 505.0220.

4.1.3.1. 2-(7-(Benzo[d]thiazol-2-ylthio)-5-(propylthio)-3H-[1,2,3]triazolo[4,5-d]pyrimidin-3-yl)ethyl benzoate (9b).

Pale yellow solid, m.p. 97–98 °C, yield 79%. ^{1}H NMR (400 MHz, CDCl$_3$) δ 8.11–8.13 (m, 1H), 7.96–7.98 (m, 1H), 7.91–7.94 (m, 2H), 7.54–7.58 (m, 2H), 7.48–7.52 (m, 1H), 7.40–7.44 (m, 2H), 5.02–5.05 (t, J = 5.2 Hz, 2H), 4.83–4.85 (t, J = 5.2 Hz, 2H), 2.87–2.90 (t, J = 7.2 Hz, 2H), 1.50–1.59 (m, 2H), 0.83–0.86 (t, J = 7.4 Hz, 3H). ^{13}C NMR (100 MHz, CDCl$_3$) δ 171.0, 166.0, 160.0, 155.3, 152.1, 149.3, 137.2, 133.4, 131.0, 129.8, 129.2, 128.5, 126.6, 125.9, 123.4, 121.3, 62.3, 46.1, 33.32, 22.1, 13.3. HR-MS (ESI): Calcd. C$_{23}$H$_{20}$N$_6$O$_2$S$_3$, [M+Na]$^+$: 531.0708, Found: 531.0709.
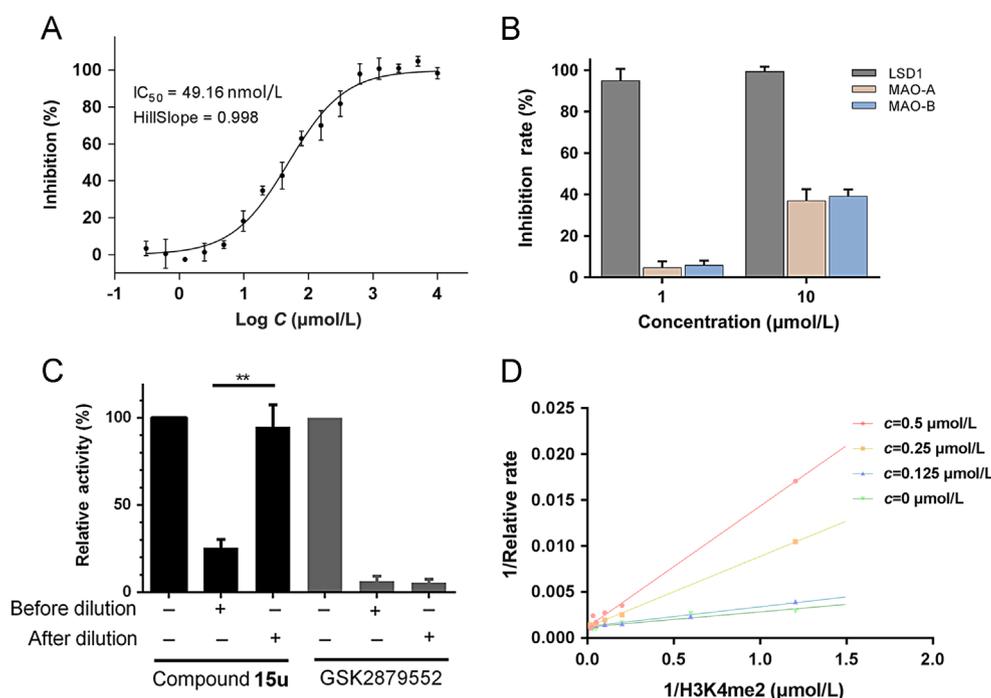
Figure 4 (A) Inhibition of compound **15u** against LSD1; (B) Inhibition of compound **15u** against LSD1 and MAO-A/B. Data are expressed as the mean of at least three determinations $\pm$ SD; (C) Compound **15u** reversibly inhibited LSD1. Data are expressed as the means $\pm$ SDs of three independent experiments; (D) Lineweaver–Burk plot of competitive inhibition for compound **15u** with indicated concentrations.
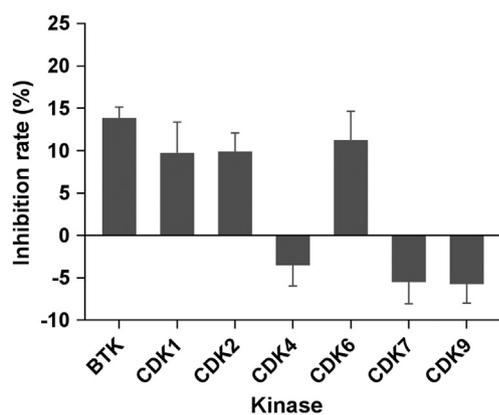

Figure 5 Inhibition of compound **15u** (10 μmol/L) against BTK and CDKs. Data are expressed as the mean of at least three determinations $\pm$ SD ($n=3$).

4.1.3.2. 2-(2-(7-(Benzo[d]thiazol-2-ylthio)-5-(propylthio)-3H-[1,2,3]triazolo[4,5-d]pyri-midin-3-yl)et-hoxy)ethyl-4-methylbenze-nesulfonate (10). White solid, m.p. 97–99 °C, yield 82%. ^{1}H NMR (400 MHz, CDCl$_3$) δ 8.12–8.14 (m, 1H), 7.97–7.99 (m, 1H), 7.76 (m, 2H), 7.55–7.59 (m, 1H), 7.48–7.53 (m, 1H), 7.35–7.37 (m, 2H), 4.72–4.75 (t, $J = 5.6$ Hz, 2H), 4.08–4.10 (t, $J = 4.6$ Hz, 2H), 4.02–4.05 (t, $J = 5.6$ Hz, 2H), 3.67–3.69 (t, $J = 4.6$ Hz, 2H), 2.99–3.02 (t, $J = 7.2$ Hz, 2H), 2.46 (s, 3H), 1.59–1.64 (m, 2H), 0.87–0.91 (t, $J = 7.2$ Hz, 3H). ^{13}C NMR (100 MHz, CDCl$_3$) δ 170.7, 159.9, 155.4, 152.2, 149.2, 144.9, 137.3, 131.0, 129.9, 127.9, 126.5, 125.9, 123.4, 121.3, 68.9, 68.8, 68.5, 68.4, 46.5, 33.5, 22.2, 13.3. HR-MS (ESI): Calcd. C$_{25}$H$_{26}$N$_6$O$_4$S$_4$, [M+H]$^+$: 603.0977, Found: 603.0975.

4.1.4. Preparation of compounds 14a–i

To a mixture of appropriate amines **11** (1 eq.), TEA or DABCO (3 eq.) in THF was added CS$_2$ (3 eq.) dropwise at rt. The precipitate was formed and the reaction was kept overnight. The dithiocarbamic acid salts **12** were readily obtained after filtration,

Table 5 Antiproliferative activity of compounds **15s**, **15u** and **15y**.

Cell line	Cell type	IC$_{50}$ (μmol/L)[a]		
		15s	**15u**	**15y**
OCI-AML3	Leukemia	2.50 ± 0.54	1.79 ± 0.14	4.72 ± 1.11
K562	Leukemia	7.02 ± 1.01	1.30 ± 0.36	7.24 ± 0.93
THP-1	Leukemia	1.14 ± 0.25	0.45 ± 0.11	2.52 ± 0.82
U937	Leukemia	2.31 ± 0.33	1.22 ± 0.31	3.23 ± 0.28
Raji	Lymphoma	3.02 ± 0.95	1.40 ± 0.49	3.32 ± 0.75

[a]Cell lines were treated with compounds for 6 days. Data are expressed as the mean $\pm$ SD of three independent experiments ($n = 3$).
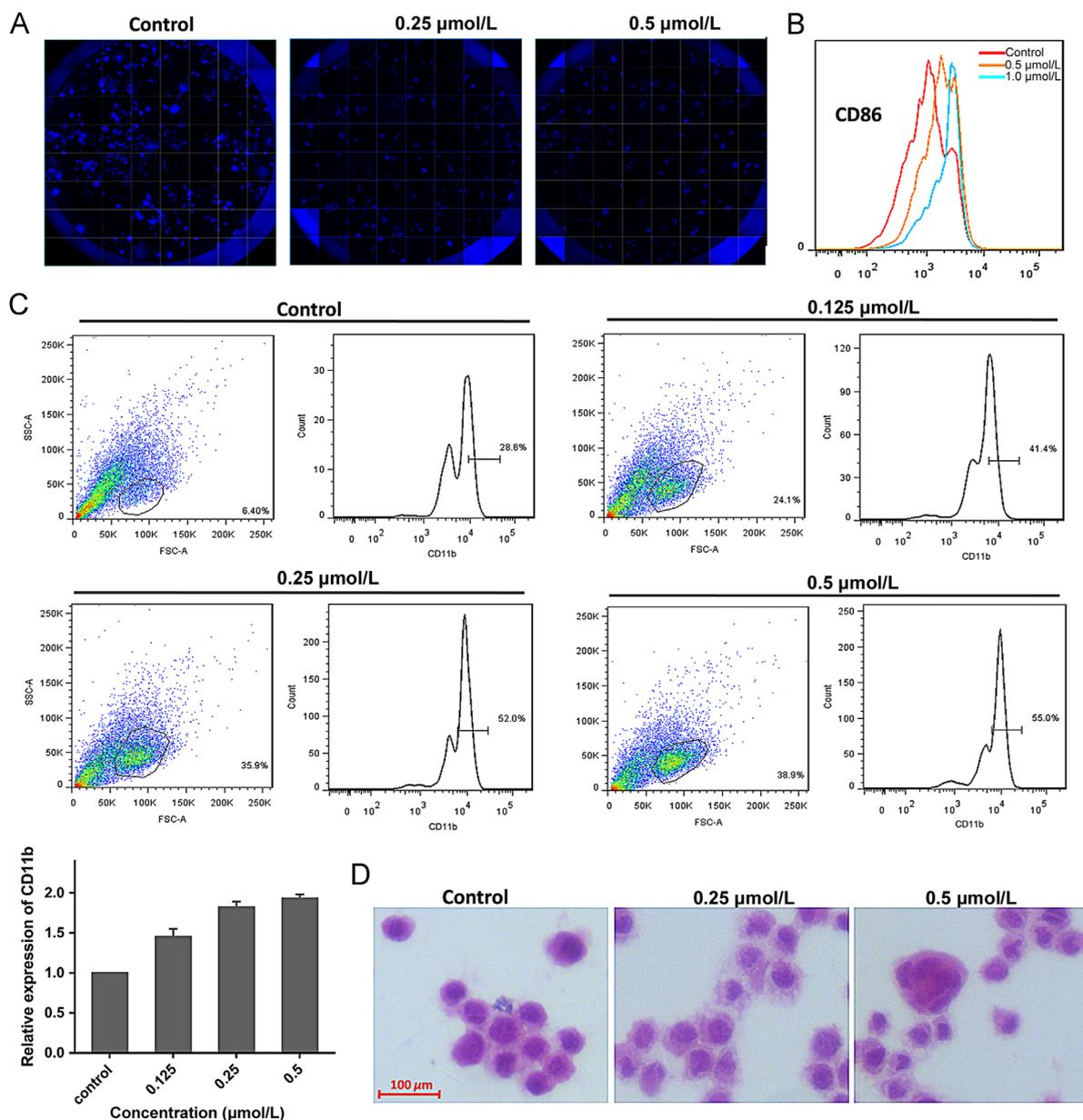
Figure 6 (A) Colony formation for THP-1 cells treated with indicated concentrations of compound **15u** for 8 days; (B) CD86 expression of THP-1 cells analyzed by flow cytometry after treatment with compound **15u** for 8 days; (C) CD11b expression of THP-1 cells analyzed by flow cytometry after treatment with compound **15u** for 8 days; (D) Cell morphology of THP-1 cells analyzed by Wright–Giemsa staining after treatment with compound **15u**.

which then reacted with triphosgene (0.5 eq) in chlorofrom at rt to form isothiocyanates **13** after a short flash column chromatography (PE as eluent). The obtained **13** was reacted with NaN_3 (3 eq.) in water under refluxing over 5 h, and then cooled down to rt. The reaction mixture was treated with aq HCl until the pH reached to 3, the formed precipitate was filtrated to give the mercapto tetrazole **14**, which was used for the next step without further purification.

4.1.5. Preparation of compound 17
To a solution of compound **4b** (450 mg, 1.9 mmol, 1.1 eq.) and phenyl isothiocyanate (230 mg, 1.7 mmol, 1 eq.) in 20 mL of acetonitrile was added Cs_2CO_3 (1.2 g, 3.7 mmol, 2.2 eq.) portion-wise at rt, and the resultant slurry was stirred overnight. After completion of the reaction, the mixture was diluted with ethyl

acetate and washed with water. The organic phase was concentrated under vacuum. The residue was purified by flash column chromatography (PE/EA = 6:1) to afford 300 mg of intermediate **16** as light yellow solid, yield: 52%. A mixture of 5-mercapto-1-methyltetrazole (50 mg, 0.43 mmol, 1 eq.), compound **16** (146 mg, 0.43 mmol, 1 eq.) and K_2CO_3 (60 mg, 0.43 mmol, 1 eq.) in 20 mL of isopropanol was refluxed and monitored by TLC (PE/EA = 5:1). After 5 h, the reaction was done, and then the slurry was filtrated over celite pad. The filtrate was concentrated under vacuum, and the residue was purified by flash column chromatography to give compound **17**, white solid, yield: 68% (120 mg), m.p. 240–241 °C. ^{1}H NMR (400 MHz, DMSO-d_6) δ 11.09 (s, 1H), 7.72–7.74 (m, 2H), 7.42–7.45 (m, 2H), 7.11–7.15 (m, 1H), 4.09 (s, 3H), 3.35 (s, 2H), 2.61–2.65 (t, J = 7.2 Hz, 2H), 1.34–1.41 (m,

2H), 0.84–0.88 (t, $J = 7.3$ Hz, 3H). ^{13}C NMR (100 MHz, DMSO-d_6) δ 162.4, 161.8, 159.7, 149.6, 146.6, 139.4, 137.5, 129.2, 123.4, 118.4, 34.6, 32.3, 22.0, 13.0. HR-MS (ESI): Calcd. C$_{16}$H$_{16}$N$_8$S$_3$, [M+Na]$^+$: 439.0558, Found: 439.0554.

4.1.6. Preparation of compound 19

A mixture of compound **6j** (100 mg) and aq HCl (0.2 mL) in 5 mL of triethylorthoformate was kept overnight at rt. The resulting solid was filtrated and washed with ether, affording 60 mg of intermediate **18** (yield: 58%). Then mixture of **18** (60 mg, 0.19 mmol, 1 eq.), 5-mercapto-1-methyltetrazole (24 mg, 0.21 mmol, 1.1 eq.) and N,N-diisopropylethylamine (50 mg, 0.39 mmol, 2 eq.) in 15 mL of DMF was heated to 100 °C for 3 h. Then the reaction mixture was cooled to rt, and diluted with ethyl acetate and washed with water for three times successively. The organic phase was concentrated under vacuum, and the residue was purified by flash column chromatography (PE/EA = 4:1) to afford 54 mg of compound **19** as off-white solid, yield: 72%, m.p. 118–120 °C. ^{1}H NMR (400 MHz, DMSO-d_6) δ 8.59 (s, 1H), 7.30–7.36 (m, 5H), 5.41 (s, 2H), 4.06 (s, 3H), 2.75–2.78 (t, $J = 7.2$ Hz, 2H), 1.42–1.48 (m, 2H), 0.86–0.90 (t, $J = 7.3$ Hz, 3H). ^{13}C NMR (100 MHz, DMSO-d_6) δ 164.1, 153.8, 150.8, 146.2, 145.4, 136.0, 128.7, 128.0, 127.9, 127.7, 46.7, 34.6, 32.4, 22.1, 13.1. HR-MS (ESI): Calcd. C$_{17}$H$_{18}$N$_8$S$_2$, [M+Na]$^+$: 421.0994, Found: 421.0995.

4.1.7. Preparation of compounds 22a–b

A solution of compound **20** (1 eq.), mercaptophenyltetrazole (1 eq.) and DIEA (1.2 eq.) in DMF was heated at 100 °C for 2 h. The reaction mixture was then cooled to rt, diluted with ethyl acetate (EA), and washed with water. The organic phase was dried over NaSO$_4$, and the solvent was removed under vacuum, and the residue was purified by flash column chromatography (PE/EA = 4:1) to afford intermediate **21**. A mixture of **21** (1 eq.), ethanolamine (1 eq.) and DIEA (1.1 eq.) in a mixed solvent of isopropanol/DMF (v/v = 1:1) was heated at 90 °C for 3 h, and then cooled to rt. The reaction mixture was concentrated under vacuum, and then poured into water and extracted with EA. The combined organic phases were dried over Na$_2$SO$_4$, filtrated, concentrated and purified by flash column chromatography (PE/EA = 1:1) to give the desired product **22**.

4.1.7.1. 2-((6-((1-Phenyl-1H-tetrazol-5-yl)thio)-2-(prop-2-yn-1-ylthio)pyrimidin-4-yl)-amino)ethan-1-ol (22a). Waxy solid, yield 72%. ^{1}H NMR (400 MHz, CDCl$_3$) δ 7.54–7.60 (m, 5H), 6.32 (s, 1H), 5.44 (br, 1H), 3.81 (t, $J = 5.0$ Hz, 2H), 3.70–3.75 (m, 1H), 3.61 (d, $J = 2.6$ Hz, 2H), 3.55 (br, 1H), 2.08 (t, $J = 2.6$ Hz, 1H).

4.1.7.2. 2-((2-(Benzylthio)-6-((1-phenyl-1H-tetrazol-5-yl)thio)pyrimidin-4-yl)amino)ethan-1-ol (22b). Light yellow oil, yield 65%. ^{1}H NMR (400 MHz, CDCl$_3$) δ 7.50–7.53 (m, 5H), 7.19–7.28 (m, 5H), 6.24 (s, 1H), 5.66–5.69 (t, $J = 5.7$ Hz, 1H), 4.11 (s, 2H), 3.71–3.74 (t, $J = 5.0$ Hz, 2H), 3.47 (m, 2H). ^{13}C NMR (100 MHz, CDCl$_3$) δ 171.0, 161.8, 148.2, 137.3, 133.4, 130.7, 129.7, 128.8, 128.5, 127.1, 124.8, 61.5, 43.5, 35.0. HR-MS (ESI): Calcd. C$_{20}$H$_{19}$N$_7$OS$_2$, [M+Na]$^+$: 460.0900, Found: 460.0991.

4.1.8. Preparation of compound 23

A mixture of **22a** (100 mg, 0.26 mmol, 1 eq.), benzyl azido (40 mg, 0.30 mmol, 1.15 eq.), sodium ascorbate (5 mg, 0.1 eq.) and CuSO$_4$ (5 mg, 0.1 eq.) in 8 mL of mixed solvent of THF/water (1:1) was stirred at rt for 3 h. The reaction mixture was diluted with EA, washed with water for three times. The organic phase

was concentrated under vacuum, and the residue was purified by flash column chromatography (PE/EA = 2:3) to give compound **23** as pale yellow solid, yield 57%. m.p. 51–53 °C, ^{1}H NMR (400 MHz, DMSO-d_6) δ 7.94 (s, 1H), 7.66–7.68 (m, 3H), 7.62 (m, 3H), 7.33–7.37 (m, 3H), 7.27–7.29 (m, 2H), 6.04 (s, 1H), 5.54 (s, 2H), 4.73–4.76 (t, $J = 5.2$ Hz, 1H), 4.15 (s, 2H), 3.42–3.45 (m, 2H), 3.30–3.31 (m, 2H). ^{13}C NMR (100 MHz, DMSO-d_6) δ 169.2, 161.4, 159.8, 147.9, 143.9, 136.0, 133.2, 130.8, 129.6, 128.7, 128.1, 127.8, 125.2, 123.2, 97.9, 59.3, 52.7, 42.7, 24.7. HR-MS (ESI): Calcd. C$_{23}$H$_{22}$N$_{10}$OS$_2$, [M+Na]$^+$: 541.1317, Found: 541.1318.

4.2. Biology assay

4.2.1. LSD1 enzymatic assay

Inhibitory effects of the target compounds against LSD1 were evaluated according to the reported methods[62]. Full length LSD1 cDNA encoding LSD1 was obtained by RT-PCR and cloned into pET-28b (pET-28b-LSD1). Then the plasmid pET-28b-LSD1 was transfected into BL21 (DE). The recombinant protein was induced with 0.25 mmol/L IPTG at 20 °C and purified following affinity chromatography, ion exchange chromatography and gel filtration. Then the compounds were incubated with the 5 nmol/L recombinant LSD1 and 25 μmol/L H3K4me2 peptide in the present of FAD (50 nmol/L), Amplex Red (20 nmol/L) and horseradish peroxidase (5.5 U/mL) for 30 min. After that, the fluorescence was measured at excitation wavelength 530 nm and emission wavelength 590 nm as reported in order to evaluate the inhibition rate of the candidate compounds. In the control experiment, assay with specific concentration of H$_2$O$_2$ coupled with Amplex Red and HRP was performed to exclude the false positive result.

For the competitive analysis of the candidate compound, the demethylase activity of LSD1 was assessed in the presence of different concentrations of the compound (0, 0.125, 0.25 and 0.5 μmol/L) at a fixed concentration of FAD (2.5 μmol/L) and peptide concentrations from 0 to 60 μmol/L. Assays were performed triplicate, and kinetics values were obtained using Lineweaver–Burk plots[63] made by GraphPad 6.0 (GraphPad Software Inc., San Diego, CA, USA).

4.2.2. Inhibitory evaluation of compound 15u against MAO-A/B

The MAO-A/B were purchased from Active Motif (Cat31502, Cat31503). Biochemical kits were purchased from Promega (MAO-Glo Assay, V1402). Inhibition assay was carried out according to the manufacturer's protocol. The tested compound solution was transferred into a 384-well plate in duplicate, then incubated with 10 μL of recombinant MAO-A or MAO-B solutions at rt for 15 min (the final concentration was 15 and 20 nmol/L respectively), followed by adding 10 μL of luciferin derivative substrate (the final concentration is 10 μmol/L) to initiate the reaction. After incubation for 60 min at rt, the reporter luciferase detection reagent (20 μL) was added and incubated with each reaction for an additional 20 min. Relative light units (RLU) were detected using plate reader.

4.2.3. BTK enzyme assay

BTK was purchased from Carna Biosciences. The kinases (5 nmol/L) were assayed with 5 μL tested compounds, 3 μmol/L peptide2 (5-FAM-EAIYAAPFAKKK), 90 μmol/L ATP, and reaction buffer (50 mmol/L HEPES, pH 7.5, 0.0015% Brij-35, 10 mmol/L MgCl$_2$, 2 mmol/L DTT). After incubation at 28 °C for 60 min, the reactions were stopped by adding 25 μL stop buffer (100 mmol/L HEPES,

pH 7.5, 0.015% Brij-35, 50 mmol/L EDTA). The reaction mixture was analyzed on Caliper, and the readout values were converted to inhibition values.

4.2.4. CDKs enzyme assay

CDK1/cyclinB, CDK2/CycA2, CDK7/cyclinH/MAT1 and CDK9/cyclinT1 kinase were purchased from Millipore, and CDK4/CycD3, CDK6/cycD3 were purchased from Carna. The kinases were assayed with 3 μmol/L peptide8 (5-FAM-IPTSPITT-TYFFFKKK-COOH for CDK4 and CDK6), peptide18 (5-FAM-QSPKKG-CONH$_2$ for CDK1 and CDK2), peptide CTD3 (5-FAM-ACSYSPTSPSYSPTSPSYSPTSPSKK for CDK7 and CDK9) in the 20/30/280/800/77/10 μmol/L ATP (for CDK1/CDK2/CDK4/CDK6/CDK7CDK9), and of the test compounds in a final volume of 5 μL, and the reaction buffer (50 mmol/L HEPES, pH 7.5, 0.0015% Brij-35, 10 mmol/L MgCl$_2$, 2 mmol/L DTT). After incubation at 28 °C for 60 min, the reactions were stopped by adding 25 μL stop buffer (100 mmol/L HEPES, pH 7.5, 0.015% Brij-35, 50 mmol/L EDTA). The reaction mixture was analyzed on Caliper, and the readout values were converted to inhibition values.

4.2.5. Reversibility analysis

The dilution assay was done as published[64]. Briefly, an amount of 2.5 μg of recombinant LSD1 was incubated with 312.5 μmol/L compound **15u** , 600 μmol/L GSK2879552, or DMSO. At 1 h later, 1.25 μL aliquots were removed from all samples and diluted into HRP-assay solution containing substrate and coupling reagents to a final volume of 100 μL. This represents an 80-fold dilution of the inhibitor concentration, which is expected to yield the same inhibition rate for an irreversible inhibitor or significant difference for a reversible inhibitor.

4.2.6. Morphological analysis

The morphological analysis of THP-1 cells differentiation, cytospins were prepared by centrifugation in 150 μL PBS at a speed of 300 rpm for 5 min. The cytospun slides were stained at rt with hematoxylin and eosin (Solarbio), and cellular morphology was examined using a microscope with a camera (Leica, Wetzlar, Germany).

4.2.7. Cell viability assay

The MTS/PMS method was used to evaluate the inhibition of cancer cell proliferation. Cells were treated with various concentrations of the test compounds. After the incubation of 6 d, MTS assay was performed using CellTiter 96® AQueous One Solution Cell Proliferation Assay (Promega, USA) according to the manufacturer's instructions. At least three independent experiments were performed for statistics. All data were represented as mean±SD, $n=3$.

4.2.8. Colony formation assay

THP-1 cells (500 cells/well) were seeded in 24-well plate, 1:1 mixture of RPMI 1640 containing 10% FBS (BI) and Methylcellulose-based medium as the culture medium. Cells were treated with compound **15u** at indicated concentrations for 8 days. Then cells were stained with DAPI (Sigma) according to the manufacturer's instructions and washed with PBS. The colony formation was analyzed using High Content analyzer (Thermo-Fisher, Waltham, MA, USA).

4.2.9. Flow-cytometry

Over 8 days of incubation with indicated concentrations of compound **15u** or 0.1% DMSO, 1×10^6 THP-1 cells were treated in the dark with PE-conjugated CD11b antibody (abcam, ab28101) or FITC-conjugated CD86 antibody (abcam, ab77131) at 4 °C for 30 min. The expression of CD11b and CD86 was analyzed by FACSCanto™II flow cytometer (BD Biosciences, San Jose, CA, USA) and the flow cytometry data was analyzed using Flowjo.

4.3. Molecular modeling simulations and docking simulations

The structures of the studied ligands were built up by MOE 2015.10 and minimized using Amber10:EHT force field. The crystal structure of LSD1 in complex with an H3K4 peptide (PDB code: 2V1D) was prepared by QuickPrep module using the default parameters. The H3K4 peptide binding pocket was set as the docking site in this study. Induced fit docking simulations were carried out to predict the possible interactions for the receptor–ligand system using the Dock module of MOE 2015.10. During the docking simulations, all the side chains of residues surrounding the defined binding site were regarded as rotatable bonds, and the ligand and its single bonds were allowed to move freely within the potential binding pocket. After the docking simulations, the 20 best-scored ligand–protein complexes of each ligand were kept for further analyses. The result of our induced fit docking simulations showed that the best-scored conformations of our ligands were similar. Therefore, only the LSD1–ligand complex of the most active compound **15u** was selected to analyze the interaction mode.

Appendix A. Supporting information

Supporting data associated with this article can be found in the online version at https://doi.org/10.1016/j.apsb.2019.01.001.

References

1. Kooistra SM, Helin K. Molecular mechanisms and potential functions of histone demethylases. *Nat Rev Mol Cell Biol* 2012;**13**:297–311.
2. Niu Y, Wan A, Lin Z, Lu X, Wan G. N^6-methyladenosine modification: a novel pharmacological target for anti-cancer drug development. *Acta Pharm Sin B* 2018;**8**:833–43.
3. Greer EL, Shi Y. Histone methylation: a dynamic mark in health, disease and inheritance. *Nat Rev Genet* 2012;**13**:343–57.

4. Lohse B, Kristensen JL, Kristensen LH, Agger K, Helin K, Gajhede M, et al. Inhibitors of histone demethylases. *Bioorg Med Chem* 2011;**19**:3625–36.

5. McAllister TE, England KS, Hopkinson RJ, Brennan PE, Kawamura A, Schofield CJ. Recent progress in histone demethylase inhibitors. *J Med Chem* 2016;**59**:1308–29.

6. Paik WK, Kim S. Enzymatic demethylation of calf thymus histones. *Biochem Biophys Res Commun* 1973;**51**:781–8.

7. Shi Y, Lan F, Matson C, Mulligan P, Whetstine JR, Cole PA, et al. Histone demethylation mediated by the nuclear amine oxidase homolog LSD1. *Cell* 2004;**119**:941–53.

8. Metzger E, Wissmann M, Yin N, Müller JM, Schneider R, Peters AH, et al. LSD1 demethylates repressive histone marks to promote androgen-receptor-dependent transcription. *Nature* 2005;**437**:436–9.

9. Garcia-Bassets I, Kwon YS, Telese F, Prefontaine GG, Hutt KR, Cheng CS, et al. Histone methylation-dependent mechanisms impose ligand dependency for gene activation by nuclear receptors. *Cell* 2007;**128**:505–18.

10. Wang J, Hevi S, Kurash JK, Lei H, Gay F, Bajko J, et al. The lysine demethylase LSD1 (KDM1) is required for maintenance of global DNA methylation. *Nat Genet* 2009;**41**:125–9.

11. Ooi SK, Qiu C, Bernstein E, Li K, Jia D, Yang Z, et al. DNMT3L connects unmethylated lysine 4 of histone H3 to *de novo* methylation of DNA. *Nature* 2007;**448**:714–7.

12. Ciccone DN, Su H, Hevi S, Gay F, Lei H, Bajko J, et al. KDM1B is a histone H3K4 demethylase required to establish maternal genomic imprints. *Nature* 2009;**461**:415–8.

13. Huang J, Sengupta R, Espejo AB, Lee MG, Dorsey JA, Richter M, et al. p53 is regulated by the lysine demethylase LSD1. *Nature* 2007;**449**:105–8.

14. Kontaki H, Talianidis I. Lysine methylation regulates E2F1-induced cell death. *Mol Cell* 2010;**39**:152–60.

15. Rudolph T, Yonezawa M, Lein S, Heidrich K, Kubicek S, Schäfer C, et al. Heterochromatin formation in *Drosophila* is initiated through active removal of H3K4 methylation by the LSD1 homolog SU(VAR) 3-3. *Mol Cell* 2007;**26**:103–15.

16. McGraw S, Vigneault C, Sirard MA. Temporal expression of factors involved in chromatin remodeling and in gene regulation during early bovine *in vitro* embryo development. *Reproduction* 2007;**133**:597–608.

17. Di Stefano L, Ji JY, Moon NS, Herr A, Dyson N. Mutation of *Drosophila* Lsd1 disrupts H3-K4 methylation, resulting in tissue-specific defects during development. *Curr Biol* 2007;**17**:808–12.

18. Wang GG, Allis CD, Chi P. Chromatin remodeling and cancer, part I: covalent histone modifications. *Trends Mol Med* 2007;**13**:363–72.

19. Di Stefano B, Collombet S, Jakobsen JS, Wierer M, Sardina JL, Lackner A, et al. C/EBPα creates elite cells for iPSC reprogramming by upregulating Klf4 and increasing the levels of Lsd1 and Brd4. *Nat Cell Biol* 2016;**18**:371–81.

20. Maes T, Mascaró C, Ortega A, Lunardi S, Ciceri F, Somervaille TC, et al. KDM1 histone lysine demethylases as targets for treatments of oncological and neurodegenerative disease. *Epigenomics* 2015;**7**:609–26.

21. Habibi E, Masoudi-Nejad A, Abdolmaleky HM, Haggarty SJ. Emerging roles of epigenetic mechanisms in Parkinson's disease. *Funct Integr Genom* 2011;**11**:523–37.

22. Kahl P, Gullotti L, Heukamp LC, Wolf S, Friedrichs N, Vorreuther R, et al. Androgen receptor coactivators lysine-specific histone demethylase 1 and four and a half LIM domain protein 2 predict risk of prostate cancer recurrence. *Cancer Res* 2006;**66**:11341–7.

23. Gao L, Alumkal J. Epigenetic regulation of androgen receptor signaling in prostate cancer. *Epigenetics* 2010;**5**:100–4.

24. Magerl C, Ellinger J, Braunschweig T, Kremmer E, Koch LK, Höller T, et al. H3K4 dimethylation in hepatocellular carcinoma is rare compared with other hepatobiliary and gastrointestinal carcinomas and correlates with expression of the methylase Ash2 and the demethylase LSD1. *Hum Pathol* 2010;**41**:181–9.

25. Wang Y, Zhang H, Chen Y, Sun Y, Yang F, Yu W, et al. LSD1 is a subunit of the NuRD complex and targets the metastasis programs in breast cancer. *Cell* 2009;**138**:660–72.

26. Lv T, Yuan D, Miao X, Lv Y, Zhan P, Shen X, et al. Over-expression of LSD1 promotes proliferation, migration and invasion in non-small cell lung cancer. *PLoS One* 2012;**7**:e35065.

27. Schulte JH, Lim S, Schramm A, Friedrichs N, Koster J, Versteeg R, et al. Lysine-specific demethylase 1 is strongly expressed in poorly differentiated neuroblastoma: implications for therapy. *Cancer Res* 2009;**69**:2065–71.

28. Lokken AA, Zeleznik-Le NJ. Breaking the LSD1/KDM1A addiction: therapeutic targeting of the epigenetic modifier in AML. *Cancer Cell* 2012;**21**:451–3.

29. Yokoyama A, Takezawa S, Schüle R, Kitagawa H, Kato S. Transrepressive function of TLX requires the histone demethylase LSD1. *Mol Cell Biol* 2008;**28**:3995–4003.

30. Ding J, Zhang ZM, Xia Y, Liao GQ, Pan Y, Liu S, et al. LSD1-mediated epigenetic modification contributes to proliferation and metastasis of colon cancer. *Br J Cancer* 2013;**109**:994–1003.

31. Højfeldt JW, Agger K, Helin K. Histone lysine demethylases as targets for anticancer therapy. *Nat Rev Drug Discov* 2013;**12**:917–30.

32. Sareddy GR, Viswanadhapalli S, Surapaneni P, Suzuki T, Brenner A, Vadlamudi RK. Novel KDM1A inhibitors induce differentiation and apoptosis of glioma stem cells *via* unfolded protein response pathway. *Oncogene* 2017;**36**:2423–34.

33. He Y, Zhao Y, Wang L, Bohrer LR, Pan Y, Wang L, et al. LSD1 promotes S-phase entry and tumorigenesis *via* chromatin co-occupation with E2F1 and selective H3K9 demethylation. *Oncogene* 2018;**37**:534–43.

34. Somervaille T, Salamero O, Montesinos P, Willekens C, Simon JA, Pigneux A, et al. Safety, phamacokinetics (PK), pharmacodynamics (PD) and preliminary activity in acute leukemia of Ory-1001, a first-in-Class inhibitor of lysine-specific histone demethylase 1A (LSD1/KDM1A): initial results from a first-in-human phase 1 study. *Blood* 2016;**128**:4060.

35. Zheng YC, Yu B, Chen ZS, Liu Y, Liu HM. TCPs: privileged scaffolds for identifying potent LSD1 inhibitors for cancer therapy. *Epigenomics* 2016;**8**:651–66.

36. Lee SH, Liu XM, Diamond M, Dostalik V, Favata M, He C, et al. The evaluation of INCB059872, an FAD-directed inhibitor of LSD1, in preclinical models of human small cell lung cancer. *Cancer Res* 2016;**76**:4704.

37. Fu X, Zhang P, Yu B. Advances toward LSD1 inhibitors for cancer therapy. *Future Med Chem* 2017;**9**:1227–42.

38. Mould DP, McGonagle AE, Wiseman DH, Williams EL, Jordan AM. Reversible inhibitors of LSD1 as therapeutic agents in acute myeloid leukemia: clinical significance and progress to date. *Med Res Rev* 2015;**35**:586–618.

39. Sorna V, Theisen ER, Stephens B, Warner SL, Bearss DJ, Vankayalapati H, et al. High-throughput virtual screening identifies novel *N'*-(1-phenylethylidene)-benzohydrazides as potent, specific, and reversible LSD1 inhibitors. *J Med Chem* 2013;**56**:9496–508.

40. Hitchin JR, Blagg J, Burke R, Burns S, Cockerill MJ, Fairweather EE, et al. Development and evaluation of selective, reversible LSD1 inhibitors derived from fragments. *MedChemComm* 2013;**4**:1513–22.

41. Mould DP, Alli C, Bremberg U, Cartic S, Jordan AM, Geitmann M, et al. Development of (4-cyanophenyl)glycine derivatives as reversible inhibitors of lysine specific demethylase 1. *J Med Chem* 2017;**60**:7984–99.

42. Johnson NW. The identification of GSK2879552, a mechanism based irreversible inhibitor of the histone lysine demethylase LSD1. In: XXIV EFMC international symposium on medicinal chemistry. Manchester, UK. Cambridge: Royal society of chemsitry; Aug 28–Sep 1 2016.

43. Zheng YC, Duan YC, Ma JL, Xu RM, Zi X, Lv WL, et al. Triazole-dithiocarbamate based selective lysine specific demethylase 1 (LSD1) inactivators inhibit gastric cancer cell growth, invasion, and migration. *J Med Chem* 2013;**56**:8543–60.

44. Ma LY, Zheng YC, Wang SQ, Wang B, Wang ZR, Pang LP, et al. Design, synthesis, and structure–activity relationship of novel LSD1

inhibitors based on pyrimidine-thiourea hybrids as potent, orally active antitumor agents. *J Med Chem* 2015;**58**:1705–16.

45. Ye XW, Zheng YC, Duan YC, Wang MM, Yu B, Ren JL, et al. Synthesis and biological evaluation of coumarin-1,2,3-triazole-dithio-carbamate hybrids as potent LSD1 inhibitors. *MedChemComm* 2014;**5**:650–4.

46. Li ZH, Liu XQ, Geng PF, Suo FZ, Ma JL, Yu B, et al. Discovery of [1,2,3]triazolo[4,5-*d*]pyrimidine derivatives as novel LSD1 inhibitors. *ACS Med Chem Lett* 2017;**8**:384–9.

47. Wang S, Zhao LJ, Zheng YC, Shen DD, Miao EF, Qiao XP, et al. Design, synthesis and biological evaluation of [1,2,4]triazolo[1,5-*a*] pyrimidines as potent lysine specific demethylase 1 (LSD1/KDM1A) inhibitors. *Eur J Med Chem* 2017;**125**:940–51.

48. Li ZH, Yang DX, Geng PF, Zhang J, Wei HM, Hu B, et al. Design, synthesis and biological evaluation of [1,2,3]triazolo[4,5-*d*]pyrimidine derivatives possessing a hydrazone moiety as antiproliferative agents. *Eur J Med Chem* 2016;**124**:967–80.

49. Wong R, Dolman SJ. Isothiocyanates from tosyl chloride mediated decomposition of in situ generated dithiocarbamic acid salts. *J Org Chem* 2007;**72**:3969–71.

50. Lima LM, Barreiro EJ. Bioisosterism: a useful strategy for molecular modification and drug design. *Curr Med Chem* 2005;**12**:23–49.

51. Zhao H. Scaffold selection and scaffold hopping in lead generation: a medicinal chemistry perspective. *Drug Discov Today* 2007;**12**:149–55.

52. Baell JB, Holloway GA. New substructure filters for removal of pan assay interference compounds (PAINS) from screening libraries and for their exclusion in bioassays. *J Med Chem* 2010;**53**:2719–40.

53. Vymětalová L, Kryštof V. Potential clinical uses of CDK inhibitors: lessons from synthetic lethality screens. *Med Res Rev* 2015;**35**:1156–74.

54. Shi Q, Tebben A, Dyckman AJ, Li H, Liu C, Lin J, et al. Purine derivatives as potent Bruton's tyrosine kinase (BTK) inhibitors for autoimmune diseases. *Bioorg Med Chem Lett* 2014;**24**:2206–11.

55. Cicenas J, Valius M. The CDK inhibitors in cancer research and therapy. *J Cancer Res Clin Oncol* 2011;**137**:1409–18.

56. Harris WJ, Huang X, Lynch JT, Spencer GJ, Hitchin JR, Li Y, et al. The histone demethylase KDM1A sustains the oncogenic potential of MLL-AF9 leukemia stem cells. *Cancer Cell* 2012;**21**:473–87.

57. Fang J, Ying H, Mao T, Fang Y, Lu Y, Wang H, et al. Upregulation of CD11b and CD86 through LSD1 inhibition promotes myeloid differentiation and suppresses cell proliferation in human monocytic leukemia cells. *Oncotarget* 2017;**8**:85085–101.

58. Feng Z, Yao Y, Zhou C, Chen F, Wu F, Wei L, et al. Pharmacological inhibition of LSD1 for the treatment of MLL-rearranged leukemia. *J Hematol Oncol* 2016;**9**:24.

59. McGrath JP, Williamson KE, Balasubramanian S, Odate S, Arora S, Hatton C, et al. Pharmacological inhibition of the histone lysine demethylase KDM1A suppresses the growth of multiple acute myeloid leukemia subtypes. *Cancer Res* 2016;**76**:1975–88.

60. Schenk T, Chen WC, Göllner S, Howell L, Jin L, Hebestreit K, et al. Inhibition of the LSD1 (KDM1A) demethylase reactivates the all-*trans*-retinoic acid differentiation pathway in acute myeloid leukemia. *Nat Med* 2012;**18**:605–11.

61. Fiskus W, Sharma S, Shah B, Portier BP, Devaraj SG, Liu K, et al. Highly effective combination of LSD1 (KDM1A) antagonist and pan-histone deacetylase inhibitor against human AML cells. *Leukemia* 2014;**28**:2155–64.

62. Culhane JC, Wang DQ, Yen PM, Cole PA. Comparative analysis of small molecules and histone substrate analogues as LSD1 lysine demethylase inhibitors. *J Am Chem Soc* 2010;**132**:3164–76.

63. Lineweaver H, Burk D. The determination of enzyme dissociation constants. *J Am Chem Soc* 1934;**56**:658–66.

64. Willmann D, Lim S, Wetzel S, Metzger E, Jandausch A, Wilk W, et al. Impairment of prostate cancer cell growth by a selective and reversible lysine-specific demethylase 1 inhibitor. *Int J Cancer* 2012;**131**:2704–9.